10 Large-Scale Human Intervention and Estimation of Flood Susceptibility Applying Frequency Ratio Model

Meelan Chamling, Biswajit Bera, and Sudipa Sarkar

Abstract

Extreme weather events induced by rapid climatic change owing to irrational anthropogenic actions in recent times have dramatically increased the frequency and severity of floods across the world. Modeling the flood susceptible zones provide the much-needed requisite sustainable tool to prevent and mitigate the flood occurrence and its possible adversity on human society. The fundamental objective of the present study is to investigate the application of Frequency Ratio (FR) model in estimating the flood susceptibility areas of Torsa river basin located at the eastern Himalayan Foreland Basin. Flood inventory data of 100 flooding locations for 2017–2019 is collected from National Disaster Management Plan and processed in ArcGIS 10.3 platform to prepare the flood inventory map with 70% training and 30% validation. Eleven major flood causative factors such as altitude, geology, slope angle, slope aspect, rainfall, drainage density, plan curvature, distance from river, soil type, topographic wetness index, and land use and land cover are extracted from SRTM DEM with 30 m spatial resolution. Each individual causative parameter is processed in ArcGIS 10.3 software to prepare individual causative maps for acquiring the essential values of fluvio-hydrological and spatiotemporal features of flooding parameters mandatory for the calculation of F.R model. The flood susceptibility map computed on the basis F.R model is finally validated using Receiver Operating Characteristics (ROC) curve method to measure its scientific temperaments such as accuracy and efficiency. The estimated ROC curve value for Frequency Ratio (F.R) model is 0.92 which is considerably good and reliable for flood susceptibility determination. The model depicts that around 12 blocks are susceptible to flooding events in the district of Alipurduar and Cooch Behar district of Terai-dooars region. In Alipurduar district nearly 11.01% of people are vulnerable to flood while in Cooch Behar district it is about 3.79%. Most of these blocks and their people are highly exposed to flood and other fluvio-hydrological hazards.

Keywords

Torsa river system · Himalayan foreland basin · Frequency ratio (F.R) model · ROC

M. Chamling · B. Bera (✉) · S. Sarkar
Department of Geography, Sidho-Kanho-Birsha University, Ranchi Road, Purulia, India

B. Pradhan et al. (eds.), *Spatial Modelling of Flood Risk and Flood Hazards*, GIScience and Geo-environmental Modelling, https://doi.org/10.1007/978-3-030-94544-2_10

10.1 Introduction

Flood is a natural persuasive phenomenon defined by the inundation and overflow of water from the surrounding streams, rivers, lakes, aquifers, estuaries, and reservoirs to the contiguous areas that usually remain unsubmerged (Fattorelli et al. 1999). Flood is generally the outcome of a complex geological and hydro-geomorphological environment and often epitomizes the most intimidating and outrageous natural disaster of global scale owing to its rampant adversity in terms of destruction to life and property (Gashaw and Legesse 2011). Though the flood occurrence and its decimating impact are inevitable, yet the rational scientific evaluation and management of flooding events along with its causes and repercussion can be dealt with the adaptation of radically relevant analysis and forecasting methods (Cloke and Pappenberger 2009; Tehrany et al. 2015). Ascertaining the flood hazard zone and computing flood susceptibility maps will certainly become an imperious tool in preventing, managing, and mitigating the flooding prevalence and its prospective hostile imprints on the human society.

Generally, flood management methods are broadly divided into three segments viz. pre-flood measures, flood event forecast, and post-flood response (Kourgialas and Karatzas 2011). Flood management can usually be accomplished by integrating the anticipation, preparation, prevention, and evaluation of destruction (Konadu and Fosu 2009). Such critically acclaimed flood management programs can be conceivable only through the effective determination of flood susceptibility areas (Tehrany et al. 2013). The accurate and consistent identification of flood-prone areas and preparation of flood susceptibility maps enables the prompt response, diminishes the probable adversity of flood hazard, and thereby present a scientific means of early warning or caution (Kia et al. 2012).

Effective neutralization of flooding adversity through rational and scientific flood modeling is the paramount attribute of the formulation of comprehensive watershed management (Rahmati et al. 2016). Forecasting of flood events by determining the flood susceptible areas are relatively challenging owing to the lack of availability of specific and reliable hydrological data due to the dearth of sophisticated hydrological observation stations (Khosravi et al. 2016). In the recent time, hydrologists across the world have designed and enunciated different types of flood risk and susceptibility models formulated on the basis of the natural properties or parameters of watershed. These models are found to be reasonably successful in resolving the flood induce hazards in different parts of the world (Jayakrishnan et al. 2005; Bahremand et al. 2007). In case of traditional hydrological model, the adopted methodology is simple and mostly based on linear assumption mechanism which is relatively inappropriate and irrational for the holistic studies of watershed management (Liu and De Smedt 2004). Thus, these conventional and traditional hydrological methods are somewhat incompetent and have failed to provide a comprehensive assessment of flood susceptibility (Li et al. 2012; Tehrany et al. 2014). The advent of Remote Sensing and GIS techniques in the field of Hydrological science has greatly helped the researcher and administrator to streamline various fluvio-hydrological mitigation plans to deal with the pre-hazard, during hazard, and post-hazard environmental circumstances. Frequency Ratio (F.R) model based on robust Remote Sensing and GIS manoeuvre is considered significantly competitive and highly precise in contrast to any other nonlinear multivariate models to accurately evaluate the flood susceptibility area for any regional studies(Liu and De Smedt, 2004; Pourghasemi et al. 2012; Youssef et al. 2014). Several studies carried out across the world in recent contemporary period that unveils the satisfactory result of Frequency Ratio model. For example, Naghibi et al. (2015) while using Frequency Ratio model in Moghan watershed concluded that the model is highly accurate with nearly 91.21% in flood susceptibility determination. Similarly, Jaafari et al. (2014) used Frequency Ratio (F.R) model to

demarcate and prepare the landslide susceptibility map of Caspian forest. The model yields around 89.12% of precision. In another instance, Rajsekhar et al. (2013) achieved remarkable higher accomplishment of exactitude in measuring the drought categorization, drought duration identification, and drought severity studies.

Unscientific and unreasonable practices of land use and land cover (LULC) like indiscriminate deforestation, unplanned expansion of cropland, overgrazing, uncontrolled and irrational growth of human settlement, unscientific method of mining, extension of linear infrastructure such as roadway and railway, etc., are gradually degrading the spatiotemporal homeostatic equilibrium mechanism of the watershed (Bishaw 2001; Tiwari and Chatterjee 2010). The evidence of such jeopardizing adversity is apparent in recent times manifested in the form of frequent flood events along with the longer duration of water inundation within the flood plain areas. The Torsa river basin/watershed situated in the Himalayan Foreland Basin in the Eastern Himalaya is no exception in such cases. The intense increase in channel bed elevation owing to excessive sedimentation as a result of radical LULC transformation experienced by the region in recent decades have massively caused the obstruction of active channel path and frequent change in cross valley slope (Jain and Sinha 2004; Mukhopadhyay 2014). As a result, the high rate and magnitude of river channel sedimentation along with the substantial channel migration has induced severe flood events and related repercussions (Chakraborty and Ghosh 2010). The densely populated blocks under the district of Alipurduar and Cooch Behar located in the northern edge of the state of West Bengal, India are continuously exposed to the vulnerability of recurring flood hazards particular from the adverse impact of the Torsa river and its tributaries. Every year, tens and thousands of people along with the huge natural resources are utterly devastated by the dreadful and catastrophic hydro-geomorphic hazards like floods triggered by the mighty Torsa river and its tributaries in its basin areas. Therefore, an attempt has been undertaken to make a scientific study of the Torsa river basin and determine the potential flood susceptibility areas by applying the Frequency Ratio (F.R) model.

10.2 Study Area

The study area includes the Torsa river basin located at the Eastern Himalayas foredeep basin and extents between 25°55′46″ N to 26°51′ 35″N and 89°15′ 22″ E to 89°47′ 22″ E (Fig. 10.1). It covers an area of about 3340.99 km^2 and predominantly lies in the district of Alipurduar and Cooch Behar of West Bengal, India. The Torsa river is a transboundary river originating from Tibet and flows through Tibet, India, and Bangladesh. The entire course of Torsa river extends to around 295 km, out of which 75 km is in Tibet, 80 km in Bhutan, 99 km in West Bengal, India, and 45 km in Bangladesh. The important tributaries of Torsa rivers are Holong, Chhoto Torsa, Kaljani, Napania, Gadadhar, etc. The south-easterly dipping, fast-changing dynamic landscape at the foredeep basin of Himalayas controls the entire physical units or more clearly the drainage system in this area. The basin comprises alluvial soil of recent geological formation (Holocene period) and it is characterized by the presence of numerous hydro-fluvial features like swamps, natural levees, oxbow lakes, palaeo-channels, flood plains, etc. The entire designated area which lies in the Terai-dooars belt experiences tropical monsoonal climate with temperature ranging between 23 °C in summer and 10 °C in winter. Moderate and heavy rainfall encourages extensive agricultural activities.

10.3 Methods and Materials

10.3.1 Earth Observation Data

Remotely sensed multispectral band satellite data has emerged as a cost-effective, time-saving, and highly accurate tool to inspect flood hazards (Mouat et al. 1993; Coppin and Bauer 1996; Kaiser 2009; Chamling and Bera 2020). Landsat 8 Operational Land Imager (OLI) with 30 m

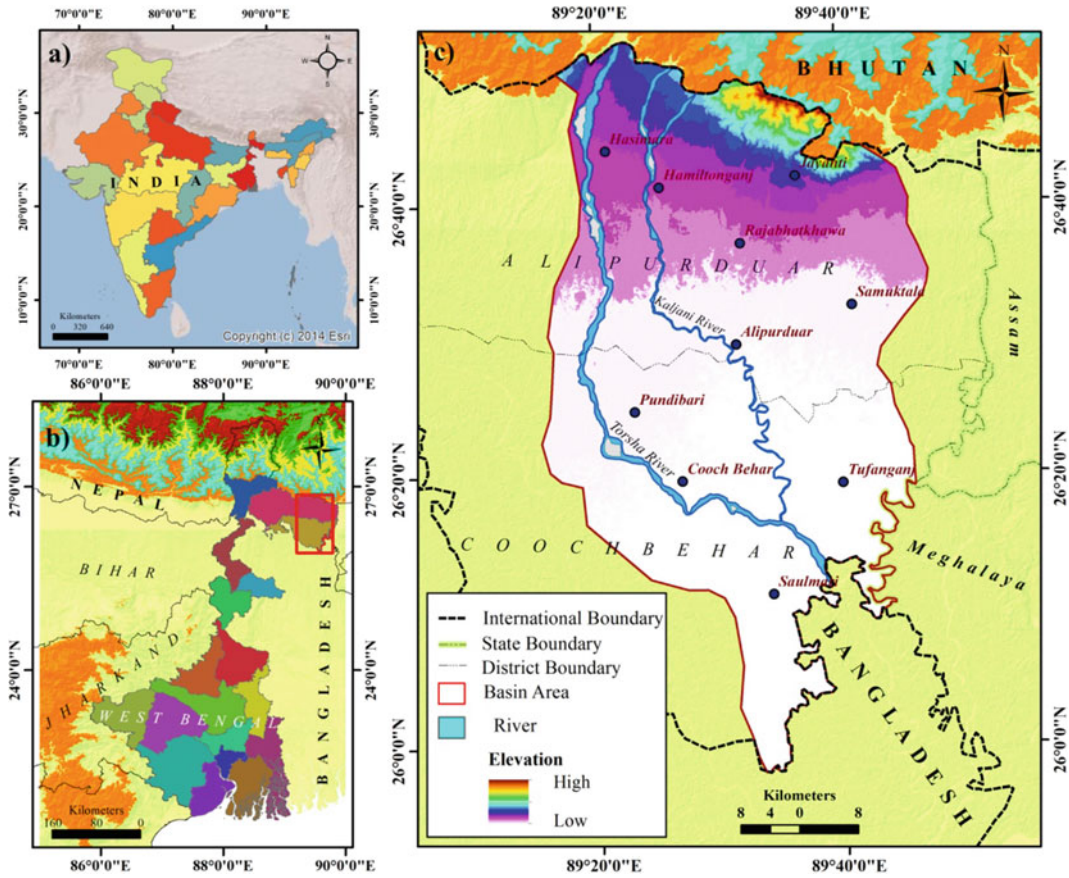

Fig. 10.1 Location of the study area

compatible spatial resolution satellite imageries are downloaded from US Geological Earth Explorer Landsat data archive (http://earthexplorer.usgs.gov/). It comprises of multi-spectral band of green (0.5 μm), red (0.6–0.7 μm), and near Infrared (1.1 μm) which is then registered in Universal Transverse Mercator (UTM) projection to prepare hybrid composite land use and land cover (LULC) classification map of study area in the ERDAS IMAGINE 2014, a raster-based geospatial software version: 16.5 (v16.5.0.852). For delineation of Torsa river watershed along with extraction of important flood causative parameters, Shuttle Radar Topography Mission (SRTM) digital elevation model (DEM) with 90 m resolution is obtained from US Geological Earth Explorer (http://earthexplorer.usgs.gov/) (Table 10.1). All the prerequisite computations of hydrological outputs are processed and executed in the ArcGIS 10.3, ESRIgeospatial software.

10.3.2 Delineation of Watershed and Extraction of Flood Causative Parameters

Torsa river basin is delineated using ArcHydro tool by exercising SRTM DEM and topographical map in ArcGIS 10.3 software following WGS 1984, UTM zone 45N projected coordinate system. Principal watershed area, drainage basin, length of river, drainage density, and drainage network with 20 m contour interval are computed and extracted employing hydrological toolset

Table 10.1 Specifications of standard data set

Sl. no.	Data type	Path/row Index/map no	Acquisition period/publication	Spatial coverage	Resolution	Source
1	SRTM DEM		2017	Alipurduar and Cooch Behar district	30 m	USGS earth explorer
2	Landsat OLI 8	139/42 139/41	2019	Alipurduar and Cooch Behar district	30 m	USGS earth explorer
3	Geological quadrangle map	78/F	2002	Alipurduar and Cooch Behar district	1:500,000	Geological survey of India
4	Topographical map	78F/7, 78F/11	1970–71	Alipurduarand Cooch Behar district	1:500,000	Survey of India
5	Soil map	Sheet no. 3	1991	Alipurduar and Cooch Behar district	1:500,000	National bureau of soil survey and land use planning
6	Meteorological	Rainfall data of 2017 is retrieved from Hasimara, Cooch Behar, Alipurduar, TufanganjNagrakata, and Banarhat submeteorological stations		Alipurduar and Cooch Behar district	–	Indian meteorological department

performed in ArcGIS 10.3 platform (Bera et al. 2019). The watershed SRTM DEM with 3,650,694 pixels having 30 m spatial resolution is analyzed in ArcGIS spatial analyst surface tool to extract slope angle and slope aspect. For identification of the major soil composition of the study area, soil map derived from National Bureau of Soil Survey (NBSS) and for demarcating the prominent lithology and geology of the region, geological map of Geological Survey of India are processed and digitized in ArcGIS 10.3 software using geographical coordinate system (WGS 1984; WKID 4326). The rainfall data is retrieved from Indian Metrological Department (IMD) local metrological substations (Table 10.1). The land use classifications are computed from multispatial band raster imageries, image interpretation, and classification process. Maximum Likelihood Classification (MLC) supervised method; a commonly used algorithm geospatial quantitative appraisal technique is used to prepare the land use categorization by performing in ERDAS IMAGINE, a raster-based geospatial software version: 16.5 (v16.5.0.852).

10.3.3 Flood Causative Conditioning Factors

To develop a strong methodology (Fig. 10.2) and to identify and evaluate the flood susceptibility, it is perquisite exercise to determine the potential causative parameters or factors and establish their relationship with flood occurrence (Liu and De Smedt 2005; Pradhan 2009). Flood susceptibility determination of any watershed relies on a large set of data as the independent variables which are effective enough to cause flooding. The processing and analyzing of such large set of causative factors in modeling process demand sufficient time and technology which often delays the quick and prompt response to flood mitigation (Campolo et al. 2003; Sanyal and Lu 2004). Considering some important parameters

and their subsequent critical analysis are required to evaluate the flood susceptibility for any region (Pradhan and Lee 2010; Skilodimou et al. 2003; Erena and Worku 2018). Therefore, eleven major flood causative factors of the Torsa river basin are considered to identify the flood susceptibility areas. These are altitude, geology, soil type, slope angle, rainfall, slope aspects, land use, drainage density, plan curvature, and topographic wetness index (TWI). The quantile method is applied to classify the each and every independent variable as each class contains similar number of features and found to be highly efficient in classification (Tehrany et al. 2013; Kia et al. 2012; Rahmati et al. 2016).

Altitude

Elevation differences always fabricate alteration in the climatic features, vegetation composition, and soil conditions (Aniya et al. 1985). Hence, altitude is one of the decisive factors in flood susceptibility mapping. The elevation map is for the designated basin using SRTM DEM with five important elevation (m) categories viz. <100, 100–200, 200–300, 300–400, and >400 (Fig. 10.3a).

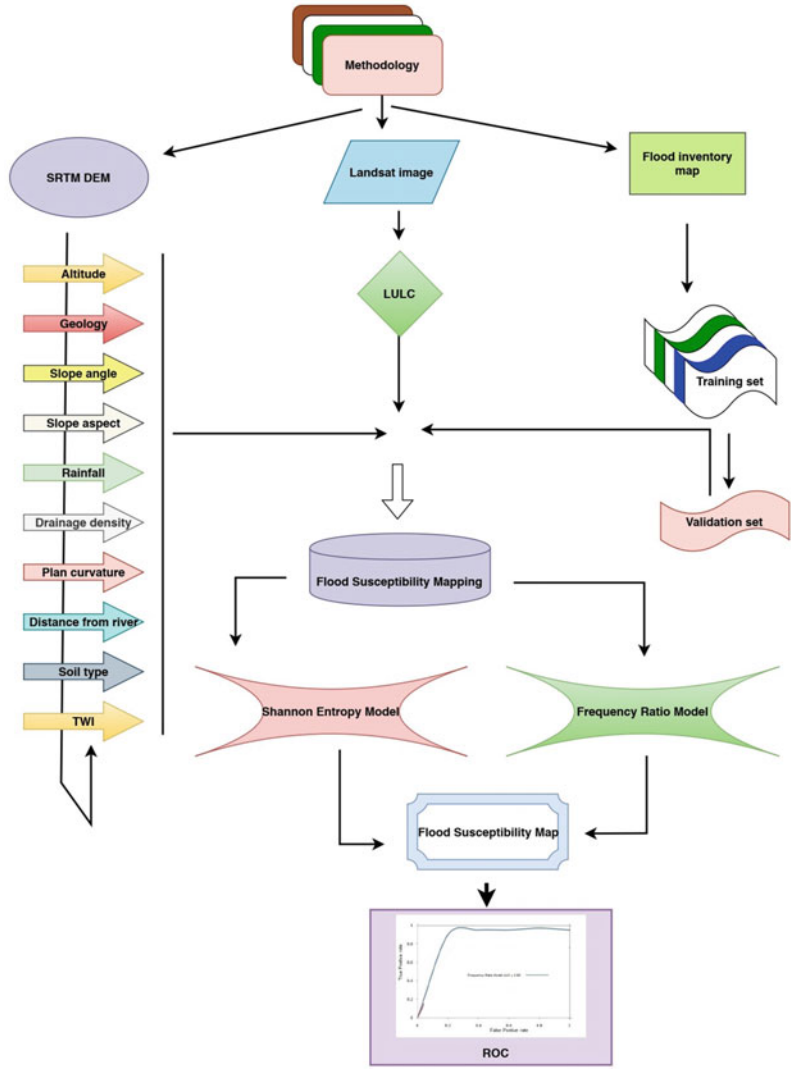

Fig. 10.2 Schematic presentation of methodology

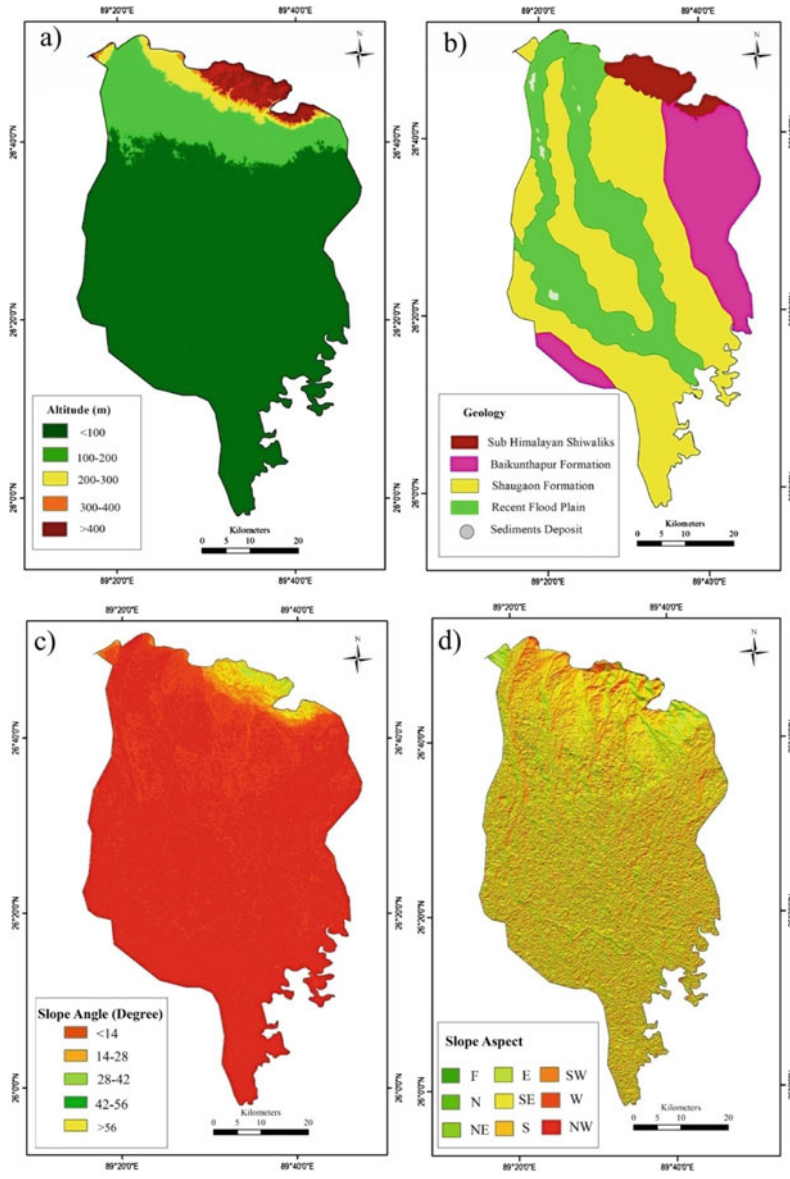

Fig. 10.3 Flood causative factors **a** Altitude **b** Geology **c** Slope angle **d** Slope aspects

Geology

Among the dominant parameters in driving the hydrological response like flood events, geology is often considered as the prominent one. The geology directly governs the flow path of surface and subsurface flow and its spatial distribution within the catchment, bedrock permeability, layers thickness, outcrop size, nature of interface between bedrocks and soil horizons, watershed water storage, etc. Drainage network, drainage density runoff, permeability power, etc., which are vital in manoeuvring the flood and it is immediately controlled by the underlying geological arrangement. Therefore, the knowledge of geological structures and their characteristic is essential in predicting flood susceptibility. The prepared geological map of selected basin area shows four major geological formations. It includes Sub Himalayan Shivalik, Baikunthapur formation, Shaogaon formation, and recent flood plain (Fig. 10.3b).

Slope Angle

Considered as one of the important factors in flood occurrence due to its direct control over surface runoff and percolation, slope angle is extracted from the SRTM DEM, and the entire study area is classified into five slope angle (°) zone viz. <2.42, 2.42–9.98, 9.98–22.39, 22.39–35.08, and >35.08 (Fig. 10.3c).

Slope Aspect

Slope aspect is a crucial parameter in evaluating the geomorphological stability by influencing the intensity of precipitation and soil moisture. To determine the water flow direction is perhaps the most important application of slope aspect computation. It is prepared in ArcGIS 10.3 software using Arc hydrological tool and classified slope into nine major direction classes. They are flat, north, south, east, west, northeast, northwest, southeast, and southwest (Fig. 10.3d).

Rainfall

The most widespread meteorological factor which leads to flooding is the amount, intensity, and duration of rainfall. The magnitude of flood is often portrayed by analyzing the peak water level during the flood by considering the various aspects of rainfall. During the monsoon season due to heavy rainfall, the rivers and lakes are frequently overburdened with additional water which results in inundation and overflow into surrounding areas. The chosen study area is divided into five rainfall zone viz. <2650, 2650–2900, 2900–3150, 3150–3400, and >3400. The computed rainfall map shows the basin receive relatively higher rainfall (Fig. 10.4a).

Drainage Density

The ratio of total length of watershed channels to the basin area is considered as drainage density. The watershed with high drainage density often triggers flashy flood hydrograph and frequent flood susceptibility. It is expressed as

$$Dd = \frac{\sum_1^n L}{A} \tag{10.1}$$

where, Dd means drainage density, L stands for length of stream, and A denotes stream basin. The selected basin is divided into six drainage density classes, namely, <0.39, 0.39–0.78, 0.78–1.17, 1.17–1.56, and >1.56 (Fig. 10.4b).

Plan Curvature

Plan curvature is an important parameter on flood probability of watershed. The curvature map processed and computed in ArcGIS. 10.3. The whole areas of basin have three important curvature plans. They are concave, flat, and convex. The Plan curvature value ranges between <2.02, 2.02–0.033, 0.33–0.45, 0.45–0.56, and >0.56 (Fig. 10.4c).

Distance from the River

Generally, flood occurs adjacent to river banks and inundates the low-lying areas of flood plains. Flood magnitude and its spatial distribution usually depend on the distance from the river. Being one of the important causative factors, distance from the river is produced based on digital layer of flow network of proximity analysis on ArcGIS software. Six flood potential classes were obtained on the basis of distance from the river. They are >500, 500–1000, 1000–1500, 1500–2000, and >2000 (Fig. 10.4d).

Soil Type

Soil plays a crucial role in influencing the runoff and subsurface characteristics in watershed and acts as a potential factor in causing flood in the downstream of the watershed. Pedological factors like soil types, characteristics, and compositions strongly determine the hydrological response to rainfall, water storage capacity, infiltration rate, and eventually the flood recurring condition. On the basis of the National Bureau of Soil Survey and Land Use Planning (NBSS& LUP), the major soil type which is

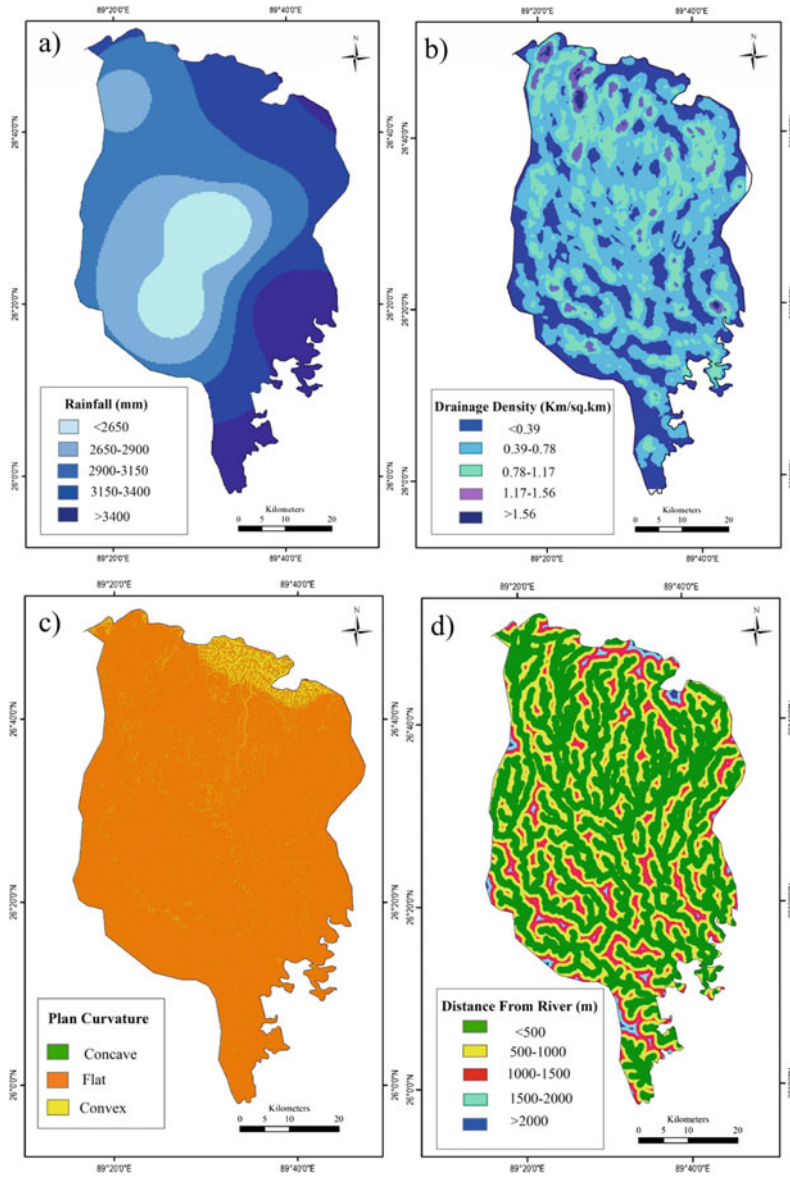

Fig. 10.4 Flood causative factor **a** Rainfall **b** Drainage density **c** Plan curvature **d** Distance from river

found in the study area and includes very fine loamy (W007) and coarse loamy soil (W008) of piedmont plain soils (Ap) and coarse loamy (W010), fine (W026) and fine silty (W028) belonging to Active alluvial plain or flood plain soils (AaA) (Fig. 10.5a).

Topographic Wetness Index (TWI)

Topographic Wetness Index (TWI) is also commonly known as compound topographic index (CTI) which is widely used to quantify the topographic or spatial scale control on

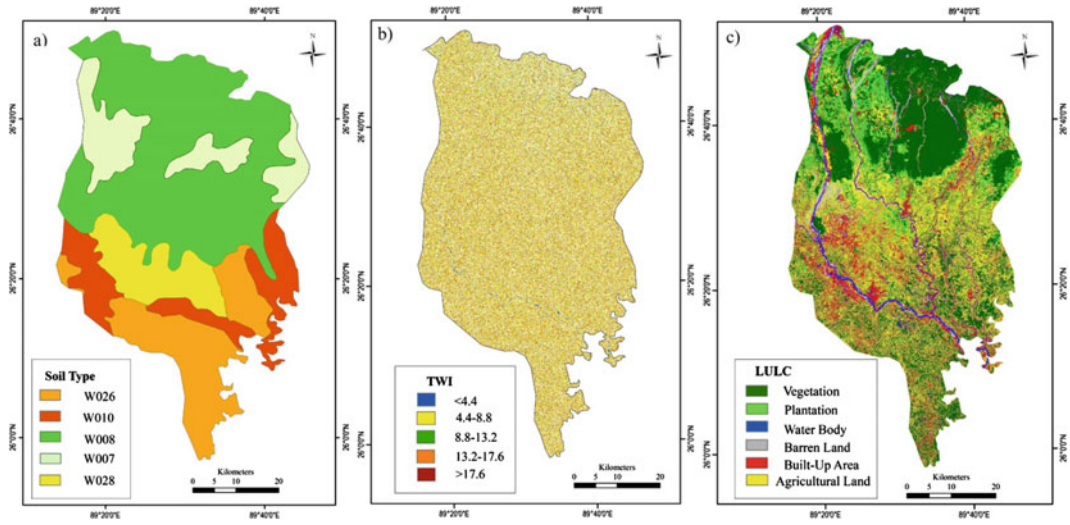

Fig. 10.5 Flood causative factor **a** Soil type **b** TWI **c** LULC

hydrological processes. It is based on the slope and upstream area which helps to identify the surface runoff flow paths and thus regarded as a significant index in examining the flood potential of any watershed. It is expressed as

$$\mathrm{TWI} = \ln\left(\frac{As}{\tan\beta}\right) \tag{10.2}$$

where, TWI means Topographic Wetness Index, As stands for specific watershed area and β denotes curvature slope (in degree). The high TWI with the value of >17.6 is randomly distributed over the basin area while the low TWI value of <4.4 lies in the extreme northern parts of the study area (Fig. 10.5b).

Land Use and Land Cover (LULC)

Land use and land cover (LULC) is an important factor in determining the hydrological condition of watershed along with topography and geology. With increasing anthropogenic activities and far and wide development and alteration of catchment area land use/cover, the incidence of flood frequency has increased many folds over the year. The land use and land cover transformation is found to be highly capable to trigger alteration of river basin hydrograph and increase the annual mean discharge, flood frequency, and overall damage. In total six LULC classes are identified in the study area namely agricultural land, built-up area, current fallow land, barren land, vegetation, and water body. The northern part of the basin area is covered with dense vegetation while the middle portion of the study area shows moderately high built-up scenario. Overall the study basin area is dominated by agricultural land with sporadic barren land (Fig. 10.5c).

10.3.4 Statistics and Mapping of Past Flood Location

In order to examine the flood potentiality, the flood inventory maps are prerequisite for the study of relationship between flood occurrence and their causative factors (Manandhar et al. 2010). The highly accurate and appropriate data of past historical flooding is obtained to create the spatial database and prepare the flood susceptibility map of the Torsa river basin. Around 100 flood location statistics that were occurred in the past from 2017 to 2019. These were collected from Disaster Management Plan of Alipurduar and Cooch Behar district and verified with intensive field survey. The specific flood events

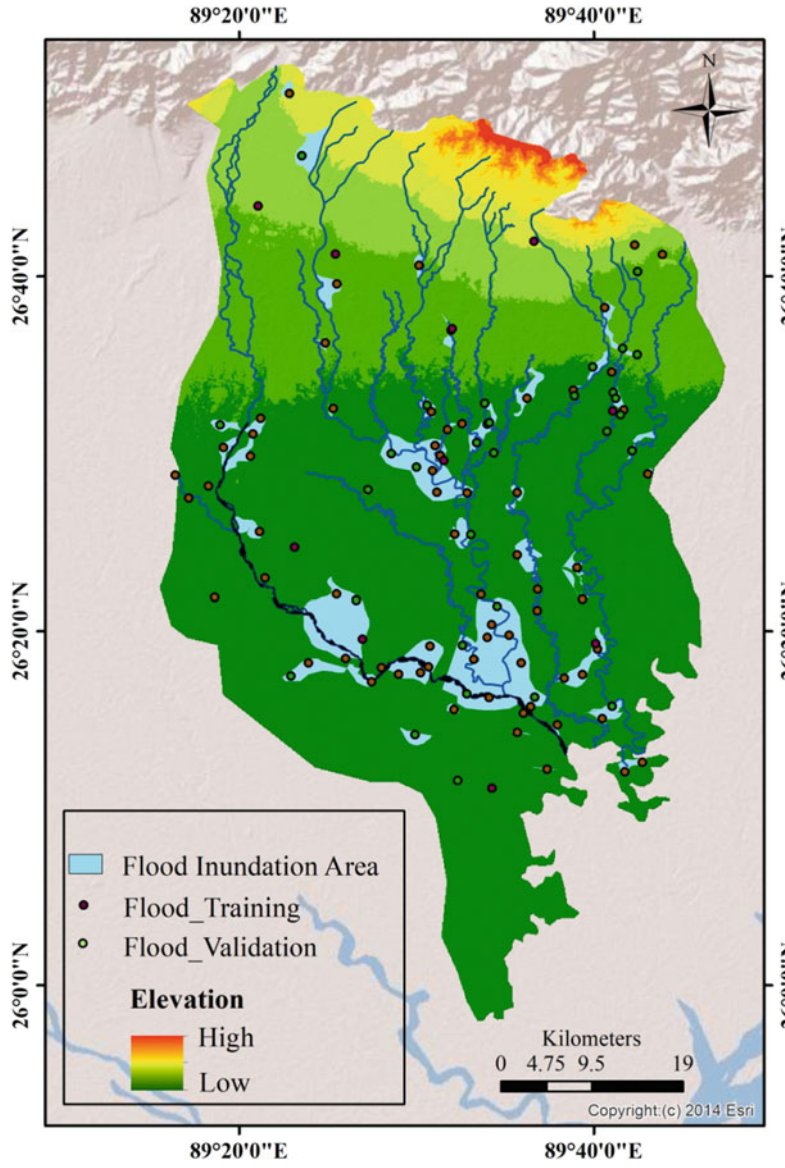

Fig. 10.6 Flood inventory map of Torsa river basin

location is used as raster network (30 × 30 m) applicable in Frequency (FR) model. Thereafter, flood inventory map is prepared using "create fishnet" technique of PNGRIS field survey, satellite dataset, disaster management database, and aftermath flooding events. 70% of total flood location points (i.e., 70 points) were randomly designated as the training data for flood modeling while the remaining 30%, i.e., 30 points were used as non-flood points for validation group on the scale of 1:25,000 (Rahmati et al. 2016) and are shown in Fig. 10.6.

10.3.5 Flood Susceptibility Modelling

10.3.5.1 Frequency Ratio (FR) Model

Frequency Ratio (F.R) model is a bivariate statistical analysis (BSA) method which facilitates the computation of probabilistic relationship

between the independent and dependent variable along with multiclassified map. It is a simple method that predicts the possibility of occurrence of certain attributes and the results can be understood with an ease (Bonham-Carter 1994; Yilmaz 2010). Past flooding events and their condition factors forms the basis for FR model. The relationship between the flood events occurrence area and the flood causative factors can be inferred from the association among the areas where the flood has not occurred and the flood causative factors. To identify the closeness of such relationship, frequency ratio approach is the highly suitable statistical technique. Frequency Ratio (F. R) model is found to be significantly effective in ranking the preferred causative factors on the basis of their capacity to influence the flood events (Kannan et al. 2013). It is expressed as

$$\mathrm{FSI} = \sum \mathrm{FR} \tag{10.3}$$

where, FSI indicates Flood Susceptibility Index while FR means frequency ratio. To compute frequency ratio, the empirical equation is used.

$$\mathrm{FR} = \frac{N_{pix}(SX_i) / \sum_{i=1}^{m} SX_i}{N_{pix}(X_j) / \sum_{j=1}^{n} (X_j)} \tag{10.4}$$

where, FR stands for Frequency Ratio, $N_{pix}(SX_i)$ indicates the number of pixels of floods within the class i of parameter variable X, $N_{pix}(X_j)$ denotes the number of pixels of parameter variable X_j, m means number of classes in parameter variable X_i, and n is the number of parameters in the area of interest (study area).

The frequency ratio (FR) is calculated for all the layers which are used in this investigation and the frequency ratio (FR) is acquired on the basis of these values (Table 10.2). Using the spatial analysis tool of ArcGIS 10.3 software, the thematic maps are reclassified and prepared.

Frequency ratio (F.R) is a reliable method which is used globally for mapping flood susceptibility and analyses the relationship of ratio between the area where the flood event occurred to the whole area of interest (Yilmaz 2009; Shafapour et al. 2019). If the FR value is found to be higher than 1, it indicates that the parameters or factors are strong enough in influencing the

Table 10.2 Determining the relationship between the flood locations and flood causative factors applying Frequency Ratio (F.R)

Factors	Class	No. of pixels in sub-basin	No. of floods	Frequency ratio (F. R)
Altitude	<100	288,963	70	1.03
	100–200	62,818	10	0.00
	200–300	29,315	0	0.00
	300–400	12,563	0	0.00
	>400	25,128	0	0.00
Geology	Sub Himalayan	117,260	29	3.02
	Shivaliks	150,763	22	0.75
	Baikunthapur	8375	10	0.06
	Formation	20,941	19	0.24
	Shaugaon Formation			
	Recent Flood Plain			
Slope angle (°)	<14	409,037	75	1.10
	14–28	8905	5	0.04
	28–42	804	0	0.00
	42–56	34	0	0.00
	>56	7	0	0.00
Slope aspect	F	39,416	3	0.55
	N	40,816	9	1.10

(continued)

Table 10.2 (continued)

Factors	Class	No. of pixels in sub-basin	No. of floods	Frequency ratio (F. R)
	NE	44,350	12	1.09
	E	53,782	10	1.06
	SE	64,797	9	1.01
	S	57,327	10	1.09
	SW	47,926	14	1.40
	W	41,376	9	1.01
	NW	28,997	4	0.61
Rainfall (mm)	<2650	123,570	5	1.01
	2650–2900	140,654	17	1.59
	2900–3150	78,504	8	0.89
	3150–3400	56,000	19	1.72
	>3400	16,019	31	2.00
Drainage density	<0.39	113,072	10	0.56
	0.39–0.78	159,139	29	1.09
	0.78–1.17	102,556	27	1.69
	1.17–1.56	37,691	8	0.90
	>1.56	6329	6	0.73
Plan curvature	Concave	142,387	0	0.00
	Flat	201,019	80	1.00
	Convex	75,381	0	0.00
Distance from river	<500	240,510	25	2.92
	500–1000	131,020	18	2.03
	1000–1500	41,212	16	1.90
	1500–2000	5385	11	0.87
	>2000	660	10	0.63
Soil type	W007	54,442	12	1.60
	W008	58,630	35	3.75
	W010	117,262	14	1.70
	W026	83,757	10	1.20
	W028	104,696	9	1.06
TWI	<4.4	203,212	30	0.80
	4.4–8.8	87,055	35	1.20
	8.8–13.2	78,321	5	1.85
	13.2–17.6	19,697	5	0.85
	>17.6	30,502	0	0.00
LULC	Vegetation	115,166	25	3.42
	Plantation	52,348	16	2.00
	Waterbody	16,751	10	1.90
	Barren land	25,127	8	1.84
	Built-up	41,880	14	1.98
	Agricultural land	167,512	7	1.00

flooding. On the other hand, if the FR is less than 1, it denotes the existence of a negative relationship between the flood event and operational variables (Lee and Talib 2005; Sujatha et al. 2013). The ratio is applied to determine the susceptibility index of the flooded area and finally, it prepares the flood susceptibility map based on frequency ratio model using empirical equation.

$$\begin{aligned} \text{FSI} = &(\text{Altitude}_{\text{FR}}) + (\text{Lithology}_{\text{FR}}) + (\text{Slope angle}_{\text{FR}}) \\ &+ (\text{Slope aspect}_{\text{FR}}) + (\text{Drainage desnity}_{\text{FR}}) \\ &+ (\text{Distance from river}_{\text{FR}}) \\ &+ (\text{Plan curvature}_{\text{FR}}) + (\text{Soil type}_{\text{FR}}) \\ &+ (\text{TWI}_{\text{FR}}) + (\text{Landuse}_{\text{FR}}) \end{aligned} \tag{10.5}$$

where, *FSI* means flood susceptibility index and *FR* is frequency ratio. The acquired pixel values are thereafter classified on the basis of natural break classification scheme (Regmi et al. 2014; Ozdemir 2011; Pourghasemi et al. 2012; Zare et al. 2013; Moghaddam et al. 2015).

10.3.5.2 Flood Susceptibility Map Validation

The application of any model depends on its accuracy and reliability which need to be validated scientifically (Akgun et al. 2008; Pradhan et al. 2009). For the present flood susceptibility map validation, the receiver operating characteristics (ROC) curve is applied to assess its suitability. The ROC curve is a simple, useful, and efficient universal method to determine the feature, indentify and predict the system (Swets 1988; Hong and Cho 2015). In ROC curve, true positive (correctly predicted pixels) rates are plotted along Y-axis while false positive (incorrectly predicted pixels) rates are shown along X-axis. To substantiate the model, area under curve (AUC) is considered. If the AUC value is 1, it indicates that the model is perfectly suitable for estimating flood susceptibility. The value of 0.5 or less means the model is inappropriate while the value greater than 0.75 denotes flood predictability is reasonably suitable (Egan 1975; Ozdemir and Altural 2013; Heagerty and Saha-Chaudhuri 2017). As per Rahmati et al. (2016), the quantitative relationship between AUC and model prediction accuracy is classified into five categories viz. poor (0.5–0.6), good (0.7–0.8), very good (0.8–0.9), and excellent (0.9–1.0). The result of ROC curve as in Fig. 10.7 reveals that AUC value of the Torsa river basin is found to be 0.92. Therefore, on the basis of computation and validation of AUC, it can be concluded that the flood susceptibility mapping of Torsa river basin is considerably accurate with FR model being a more suitable technique for identifying and mapping the flood susceptibility area.

10.4 Results and Discussion

The flood susceptibility zones or areas of Torsa river basin is determined by calculating the ten flood causative parameters or conditioning factors in Frequency Ratio model (Table 10.2). Each factor of flooding conditions is critically investigated and meticulously analyzed as flood occurrence is generally the outcome of one or

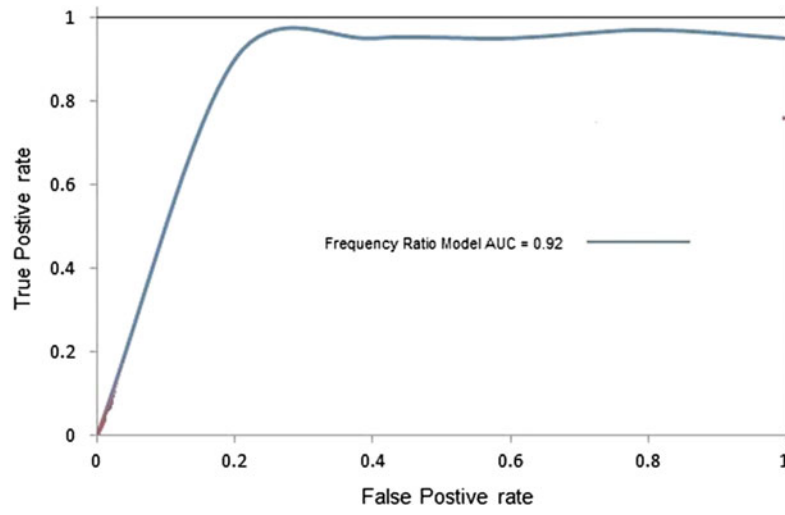

Fig. 10.7 ROC of flood susceptibility map of Torsa basin based on F.R model

more causative parameters. The scrutiny of elevation map of the basin reveals that the area with less the 100 m altitude is highly prone to flood events. These high flood susceptibility areas are spread over the entire region except in the northern parts where higher altitude is found (Fig. 10.3a). With respect to geology, recent flood plain geological formation adjacent to river banks is liable to higher flooding incidents (Fig. 10.3b). Similarly, Shaogaon formation geological sites covering the larger part of the basin is also under moderately higher vulnerable to flood (Table 10.2). The whole basin except for a small portion in the northern part lies within a low slope angle of <2.42° which portrays very high flood frequency (Fig. 10.3c). While investigating Torsa river basin, it is observed that the areas with east, south-west, west, and south-east are under high flooding events zone (Fig. 10.3d). On the other hand, land with no aspect reveals low flood (Table 10.2). In terms of rainfall, the entire basin area receives sufficiently high rainfall. Higher rainfall of more than 3150 mm and above which mostly occurs in the northern and eastern portion of the upper catchment of river Torsa provides ample discharge to cause flooding in the southern part of the basin (Fig. 10.4a). In the study area, the Plan curvature index depicts that the entire region is a flat surface which can easily lead to flooding during heavy monsoonal rainfall season (Fig. 10.4c). The computed drainage density reveals that the basin has a dense network of streams. Very high drainage density of >1.56 km^2 is randomly scattered all over the basin area which makes the southern part highly susceptible to flood (Fig. 10.4b). Distance from the river map indicates that the flood events are expected up to 2000 m away from the river. In other words, areas lying within this distance are more prone to flood than away from the 2000 m (Fig. 10.4d). The highest flood events are found within the 500–1000 m and 1000–1500 m distance away from the rivers (Table 10.2). The examination of soil type is found in the basin and it denotes that the coarse loamy soil (W008) of piedmont plain (Ap) is found in the northern and central part while at the south, fine loamy soil (W026) belonging to Active alluvial plain or flood plain soils (Aa) spreads extensively. Fine silty soil (W028) of AaA lies near the river bank. On the other hand, very fine loamy soil (W007) of Ap is scattered away near northwest and northeast of the basin. In general, the pedological factors of soils reveal that the entire basin is highly susceptible to flood (Fig. 10.5a). Topographic Wetness Index (WTI) calculation indicates that the areas with 4.4–8.8 TWI value and less than 4.4 are under high flood incidents while TWI value of 13.2–17.6 and greater than 17.6 shows no flood events (Table 10.2). Land use and land cover (LULC) map depicts high flood events in agricultural land located at the central and southern areas of the Torsa river basin (Fig. 10.5c). Most of the flooding has taken place within the flood plains which are situated close to the rivers (water body) (Table 10.2).

The Frequency Ratio model susceptibility unveils that the areas lying near the river banks are under very high flood susceptibility zones in the river Torsa basin (Fig. 10.7). High flood susceptibility areas lie just at the margin of very high flood vulnerable zones. Low and very low flood-prone areas are scattered particularly at the outer parts. Flooding events with moderate magnitude are spatially found over the whole of the basin at the periphery areas of high flooding zones (Fig. 10.8).

Around six blocks each in the district of Alipurduar and Cooch Behar of Tera-dooars region of Himalayan foredeep basin is situated within the Torsa river basin (Fig. 10.9). In case of Alipurduar district, the six blocks/municipalities are Alipurduar-I, Alipurduar-II, Kalchini, Kumargram, Madarrihat-Birpara, and Alipurduar municipality. Alipuruduar municipality with six wards is highly vulnerable as 31.37% of its populations are affected by the flooding events. Similarly, Kumargram and Alipurduar-II blocks are also under threat to high frequency of flood occurrence as nearly 22.42% and 22.165% of the populations are susceptible to flood, respectively (Table 10.3). Alipurduar-I (10.54%), Kalchini (9.91%), and Madarihat-Birpara (8.23%) blocks are relatively less susceptible. Alipurduar-II block has the highest number of affected villages (n = 41) followed by

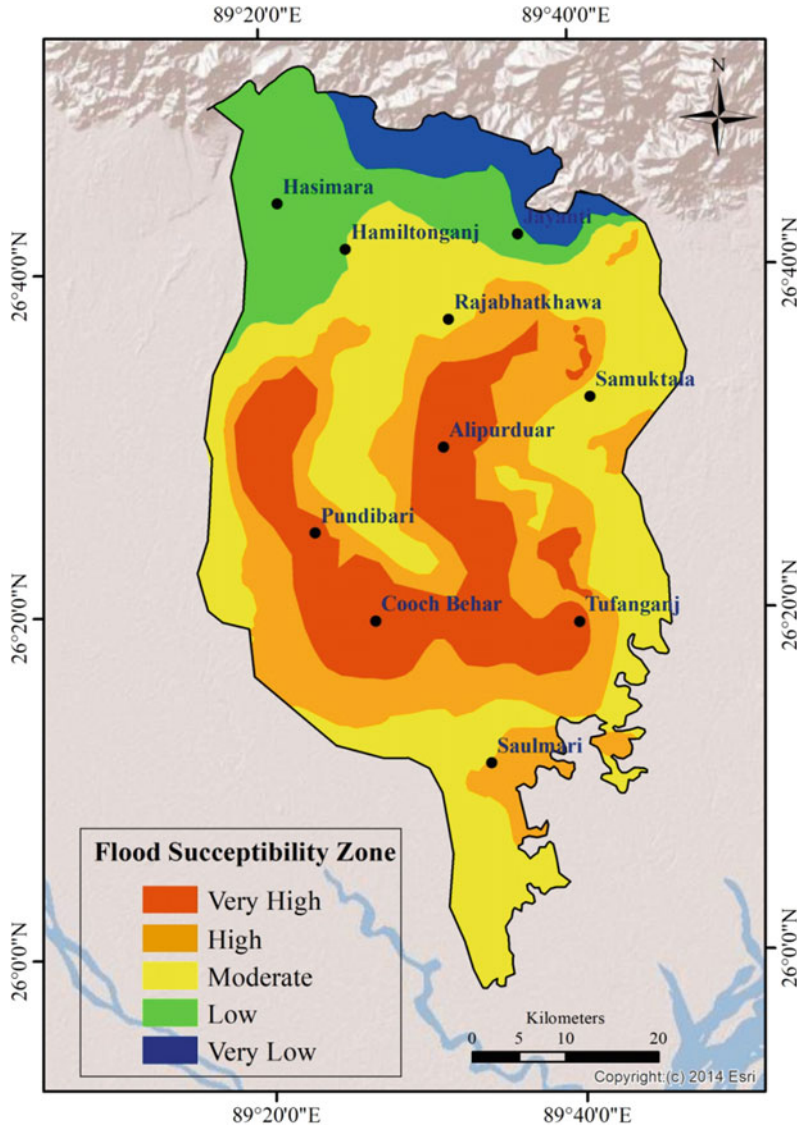

Fig. 10.8 Flood susceptibility map based on Frequency Ratio Model

Alipurduar-II (n = 28), Madarihat-Birpara (n-28), Kumargram (n = 24), and Kalchini (n = 18). In general, 11.01% of the populations of Alipurduar district is susceptible to flood occurrence and associated events caused by river Torsa and its tributaries (Table 10.3). On the other hand, in case of Cooch Behar district, nearly 3. 79% of people are exposed to havoc of floods arising from river Torsa and its associated tributaries. The people settled in six blocks of Cooch Behar-I, Cooch Behar-II, Mathabhanga-II, Tufanganj-I, Tufangaj-II, and Dinhata-II are directly affected by the flood and inundation phenomena every year during the monsoonal season. Tufanganj-I shows that largest number of vulnerable people i.e. 22.71% followed by Mathabhanga-II with 17.86%. Blocks like Tufangaj-II (4.83%), Dinhata-II (3.65%), Cooch Behar-II (3.39%), and Cooch Behar-II (1.90%) were found to be less affected by fluvio-hydrological hazards like flood. Tufanganj-I block has the highest number of villages prone to flood, i.e., n = 37. Similarly, Cooch Behar-II (n = 23) and Mathabhnaga-II (n = 20) blocks

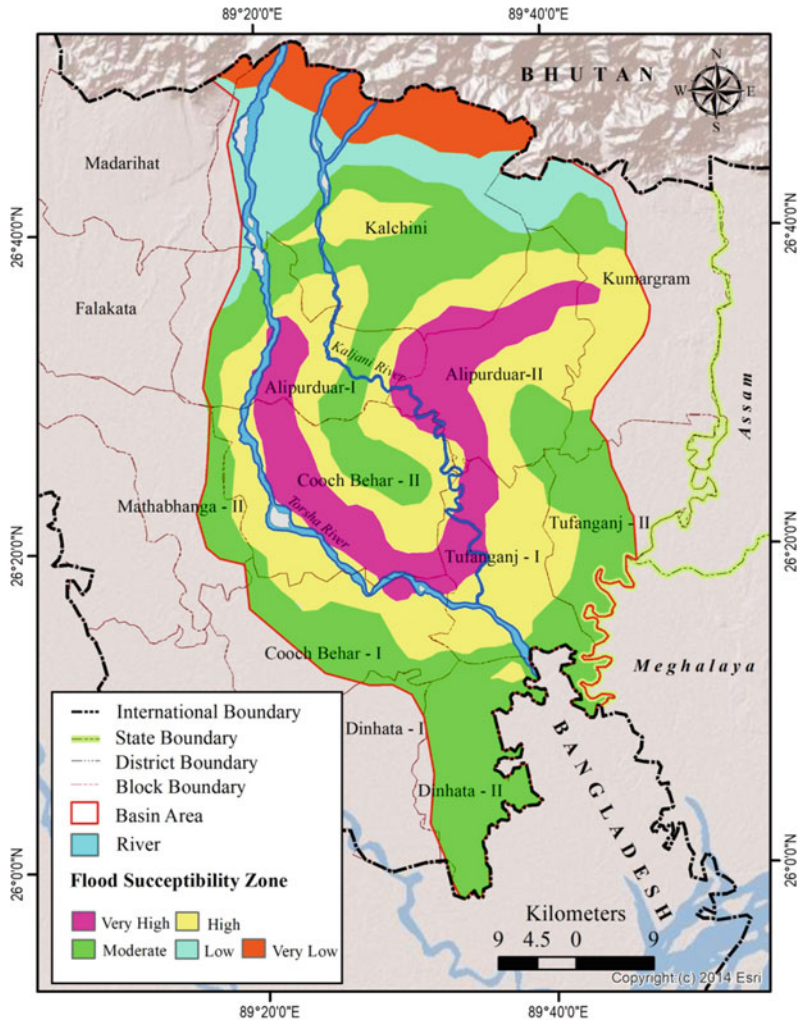

Fig. 10.9 Flood susceptible blocks and districts of Torsa river basin of Himalayan foredeep basin

also have considerably higher number of villages vulnerable to flooding. Cooch Behar-I (n = 12), Dinhata-II (n = 12), and Tufanganj-II (11) are relatively under low susceptible belts (Table 10.3).

The very high or severely affected blocks are situated along the proximity of river Torsa, Sil Torsa Kaljani, Dima, Poro, Jayanti, and Raydak-I, etc. Sil Torsa and Buri Torsa are completely detached from the main Torsa due to nodal points (off-take) avulsion. Abovementioned rivers are the tributaries of river main Torsa. Basically, Sil Torsa and Buri Torsa are the spill channels of river Torsa. Different types of avulsion took place within the Torsa river basin due to natural siltation on the channel courses and anthropogenic activities or stress on the river channels or within the river basin. River bed mining and channel bed thalweg shifting are very common fluvio-hydrological events in this fast-changing landscape. The Himalayan rivers are debouched in front of the Himalayan frontal thrust or specifically within the Himalayan foredeep basin. When Himalayan rivers enter in the foothill of the Himalayas, channel or geomorphic gradient drops suddenly. As a result, rivers become wide, sluggish, and braided in nature. National highways with railway corridors create this foredeep basin as interlacing drainage system. River Torsa and its tributaries are no exception. To mitigate

Table 10.3 Flood vulnerable statistics of Torsa river basin

District	No. of blocks	Blocks	No. of gram panchayat	Gram panchayat (GP)	Gram panchayat wise total no. of affected villages	Total no. of people affected	Blockwise % of people vulnerable to flood (Torsa river basin)	Total % of people vulnerable to flood in the district (Torsa river basin)
Alipurduar	6	Alipurduar-I	6	Pararpara Vivekananda-I Vivekananda-II PurbaKathalbari Tapshikatha Banchukumari	3 1 1 11 5 7 *n* = 28	20,800	10.54	11.01
		Alipurduar-II	5	Majherdabri Kohinoor Parokata Samuktala Mahakalguri	12 2 7 10 10 *n* = 41	43,654	22.16	
		Kalchini	6	Jaigaon Rajabathkhawa Dalsingpara Garopara Kachini Latabari	4 3 1 5 2 3 *n* = 18	25,035	9.91	
		Kumargram	5	Kumargram-Sankosh Barobisha Kamakhyaguri-I Kamakhyaguri-II Turtutikhanda	4 7 4 2 7 *n* = 24	39,921	22.42	
		Madarihat-Birpara	7	Birpara-I Birpara-II Bandapani Totopara Lankapara Hantapara Rangalibazna	1 3 6 3 3 3 9 *n* = 28	15,270	8.23	
		Alipurduar Municipality	6	Alipurduar Municipality ward no.5 Alipurduar Municipality ward no.8 Alipurduar Municipality ward no.13 Alipurduar Municipality ward no.16	*n* = 6	20,664	31.67	

(continued)

Table 10.3 (continued)

District	No. of blocks	Blocks	No. of gram panchayat	Gram panchayat (GP)	Gram panchayat wise total no. of affected villages	Total no. of people affected	Blockwise % of people vulnerable to flood (Torsa river basin)	Total % of people vulnerable to flood in the district (Torsa river basin)
				Alipurduar Municipality ward no.18 Alipurduar Municipality ward no.20				
Cooch Behar	6	Cooch Behar-I	5	Moamari Falimari Ghughumari Dawaguri Panisala	2 1 3 4 2 n = 12	5425	1.90	3.79
		Cooch Behar-II	8	Patlakhawa Madhupur Pundibari Khapaidanga Takagach Marichbari Baneswar Khagrabar	2 7 2 3 6 1 1 1 n = 23	10,112	3.39	
		Mathabhanga-II	12	Fulbari A Fulbari B Barasoulmar Ruidanga Latapata Putimari Ghoksadanga Premerdanga A.K. Paradubi Nishiganj-I Nishiganj-II Unishbisha	1 2 1 1 1 1 3 1 2 2 2 3 n = 20	35,072	17.86	
		Tufanganj-I	9	Natabari-I Maruganj Dhalpal-II Balabhut Chilakhana-I Chilakhana-II Deocharai Balarampur-I Balarampur-II	3 2 3 4 9 2 8 4 2 n = 37	50,685	22.71	
		Tufanganj-II	2	Baxirhat (Barokodali-II) Shalbari-I	3 4 4 n = 11	8090	4.83	
		Dinhata-II	2	Nazirhat-I Nazirhat-II	2 3 n = 12	7506	3.65	

the flood hazard, British ruler (since colonial period) along with Bengal landlord wanted to construct vertical concrete structures along both sides of the natural rivers. This unscientific and unrealistic approach has been practicing till today. Long stretch concrete high embankments have been built almost all the rivers within the Torsa river basin with the help of West Bengal Irrigation Department. Not only concrete high elevation embankments along with culverts, sluice gate, bridges etc. have also been constructed across the natural course of rivers. Due to unexpected population explosion along with forest land conversion, channel bed siltation is accelerating during monsoon seasons. In case of piedmont zone or Sub-Himalayan region of Bhutan–Bengal foothill zone produces a huge amount of dolomite dust and supplies to mainstream like river Torsa through its tributaries. So, flood hazard is very common recurring phenomenon in this region. Not only the abovementioned blocks of Alipurduar and Cooch Behar districts of West Bengal almost all foothill blocks are suffering due to such fluvio-hydrological hazard or disaster. During monsoon, due to shallow depth of rivers, the channel beds are cannot accommodate the huge amount of precipitated water within the channel beds and results catastrophic or devastating flood.

10.5 Conclusion

Systematic computation and scientifically sound flood susceptibility mapping of any region provide the comprehensive knowledge of prominent factors that are responsible for triggering flood events, its spatial distribution, and formulation of preventive and risk management planning. In total, eleven flood causative factors viz. altitude, geology, slope angle, slope aspect, rainfall, drainage density, plan curvature, distance from river, soil type, topographic wetness index, and land use and land cover are taken into consideration. These flood causative parameters are processed to extract the necessary fluvio-hydrological and spatiotemporal features to identify the flood susceptibility areas of Torsa river basin processed by Frequency Ratio (FR) Model in Remote Sensing environment. The Frequency Ratio (FR) Model indicates very high flood susceptibility areas located at the south and southeastern part with high vulnerable zone at the margin of very high flooding susceptible zone. Moderate flood zones are randomly distributed over the basin while low, very low flood occurrence is found in the northern and central part. In general, Frequency Ratio (FR) model identifies the Torsa river basin susceptible to frequent flooding events. The model advocates that the entire basin is prone to flood every year with more severity in the southern and southeastern areas except in the north due to the presence of higher elevation. While validating the model with receiver operating characteristics (ROC), it is found that the Frequency Ratio model is highly reliable and accurate and can be significantly used to identify and predict the flood susceptibility zones of any areas. Therefore, the model can be effectively utilized by the policymakers and planners across the world to prevent and mitigate the flooding events and their adverse damage to human society. From the colonial era, we tried to borrow the western philosophy and models to combat such devastating fluvio-hydrological hazard or disaster without getting the similarities of the hydro-geomorphological setup of the region. The anthropogenic stresses on these rivers and within this river basin indirectly invite such recurring flood hazard. The model with field validation proves the realistic situation as well as the necessity of implementation of real-time management procedures.

Acknowledgements We are grateful to the various competent authorities for providing valuable fluvio-hydrological and remote sensing data. We also express our sincere gratitude to anonymous reviewers of the journal for lending their inclusive and befitting suggestion to enhance and refurbish the standard of the research article.

Conflict of Interest The authors declared that there is no potential conflict of interest.

Ethical Statement Authors state that the research was conducted according to ethical standards.

References

Akgun A, Dag S, Bulut F (2008) Landslide susceptibility mapping for a landslide-prone area (Findikli, NE of Turkey) by likelihood-frequency ratio and weighted linear combination models. Environ Geol 54(6):1127–43. https://doi.org/10.1007/s00254-007-0882-8

Aniya M, Etaya M, Shimoda H (1985) Evaluation of Landsat data for landslide identification as a means for watershed management. J Jpn Soc Photogramm Remote Sens 24(4):17–21. https://www.jstage.jst.go.jp/article/jsprs1975/24/4/24_4_17/_pdf/-char/ja

Bahremand A, De Smedt F, Corluy J, Liu YB, Poorova J, Velcicka L, Kunikova E (2007) WetSpa model application for assessing reforestation impacts on floods in Margecany–Hornad Watershed, Slovakia. Water Resour Manag 21(8):1373–91. https://doi.org/10.1007/s11269-006-9089-0

Bera B, Bhattacharjee S, Ghosh A, Ghosh S, Chamling M (2019) Dynamic of channel potholes on Precambrian geological sites of Chhota Nagpur plateau, Indian peninsula: applying fluvio-hydrological and geospatial techniques. SN Appl Sci 21(5):1–4. https://doi.org/10.1007/s42452-019-0516-2

Bishaw B (2001) Deforestation and land degradation in the Ethiopian highlands: a strategy for physical recovery. Northeast Afr Stud 1:7–25. https://scholarworks.wmich.edu/cgi/viewcontent.cgi?article=1002&context=africancenter_icad_archive

Bonham-Carter GF (1994) Geographic information systems for geoscientists-modeling with GIS. Computer methods in the geoscientists 13:398.NII Article ID (NAID) 10016876159

Campolo M, Soldati A, Andreussi P (2003) Artificial neural network approach to flood forecasting in the River Arno. Hydrol Sci J 48(3):381–98. https://doi.org/10.1623/hysj.48.3.381.45286

Chakraborty T, Ghosh P (2010)The geomorphology and sedimentology of the Tista megafan, Darjeeling Himalaya: implications for megafan building processes. Geomorphology 115(3–4):252–6. https://doi.org/10.1016/j.geomorph.2009.06.035

Chamling M, Bera B (2020) Spatio-temporal patterns of land use/land cover change in the Bhutan–Bengal foothill region between 1987 and 2019: study towards geospatial applications and policy making. Earth Syst Environ 12:1–4. https://doi.org/10.1007/s41748-020-00150-0

Cloke HL, Pappenberger F (2009) Ensemble flood forecasting: a review. J Hydrol 375(3–4):613–26. https://doi.org/10.1016/j.jhydrol.2009.06.005

Coppin PR, Bauer ME (1996) Digital change detection in forest ecosystems with remote sensing imagery. Remote Sens Rev 13(3–4):207–34. https://doi.org/10.1080/02757259609532305

Egan JP (1975) Signal detection theory and ROC-analysis. Academic Press. ISBN-13: 978-0122328503; ISBN-10: 0122328507

Erena SH, Worku H (2018) Flood risk analysis: causes and landscape based mitigation strategies in Dire Dawa city, Ethiopia. Geoenviron Disasters 5(1):1–9. https://doi.org/10.1186/s40677-018-0110-8

Fattorelli S, Dalla Fontana G, Da Ros D (1999) Flood hazard assessment and mitigation. In Floods and landslides: integrated risk assessment. Springer, Berlin, Heidelberg, pp 19–38. https://doi.org/10.1007/978-3-642-58609-5_2

Gashaw W, Legesse D (2011) Flood hazard and risk assessment using GIS and remote sensing in Fogera Woreda, Northwest Ethiopia. In Nile River Basin. Springer, Dordrecht, pp 179–206. https://doi.org/10.1007/978-94-007-0689-7_9

Heagerty P, Saha-Chaudhuri P (2017) Time-dependent ROC curve estimation from censored survival data. 2013. R package version, 1(3).

Hong CS, Cho MH (2015) Test statistics for volume under the ROC surface and hypervolume under the ROC manifold. Commun Stat Appl Methods 22 (4):377–87. https://doi.org/10.5351/CSAM.2015.22.4.377

Jaafari A, Najafi A, Pourghasemi HR, Rezaeian J, Sattarian A (2014) GIS-based frequency ratio and index of entropy models for landslide susceptibility assessment in the Caspian forest, northern Iran. Int J Environ Sci Technol 11(4):909–926. https://doi.org/10.1007/s13762-013-0464-0

Jain V, Sinha R (2004) Fluvial dynamics of an anabranching river system in Himalayan foreland basin, Baghmati river, north Bihar plains, India 60 (1–2):147–70. https://doi.org/10.1016/j.geomorph.2003.07.008

Jayakrishnan RS, Srinivasan R, Santhi C, Arnold JG (2005) Advances in the application of the SWAT model for water resources management. Hydrol Proc Int J 19(3):749–62. https://doi.org/10.1002/hyp.5624

Kaiser MF (2009) Environmental changes, remote sensing, and infrastructure development: The case of Egypt's East Port Said harbour. Appl Geogr 29 (2):280–8. https://doi.org/10.1016/j.apgeog.2008.09.008

Kannan M, Saranathan E, Anabalagan R (2013) Landslide vulnerability mapping using frequency ratio model: a geospatial approach in Bodi-Bodimettu Ghat section, Theni district, Tamil Nadu, India. Arab J Geosci 6 (8):2901–13. https://doi.org/10.1007/s12517-012-0587-5

Khosravi K, Nohani E, Maroufinia E, Pourghasemi HR (2016) A GIS-based flood susceptibility assessment and its mapping in Iran: a comparison between frequency ratio and weights-of-evidence bivariate statistical models with multi-criteria decision-making technique. Nat Hazards 83(2):947–987. https://doi.org/10.1007/s11069-016-2357-2

Kia MB, Pirasteh S, Pradhan B, Mahmud AR, Sulaiman WN, Moradi A (2012) An artificial neural network model for flood simulation using GIS: Johor River Basin, Malaysia. Environ Earth Sci 67(1):251–64. https://doi.org/10.1007/s12665-011-1504-z

Konadu DD, Fosu C (2009). Digital elevation models and GIS for watershed modelling and flood prediction–a case study of Accra Ghana. In Appropriate technologies for environmental protection in the developing world. Springer, Dordrecht, pp 325–332. https://doi.org/10.1007/978-1-4020-9139-1_31

Kourgialas NN, Karatzas GP (2011). Flood management and a GIS modelling method to assess flood-hazard areas—a case study. Hydrol Sci J–Journal des Sciences Hydrologiques 56(2):212–25. https://doi.org/10.1080/02626667.2011.555836

Lee S, Talib JA (2005) Probabilistic landslide susceptibility and factor effect analysis. Environ Geol 47(7):982–90. https://doi.org/10.1007/s00254-005-1228-z

Li C, Singh VP, Mishra AK (2012) Entropy theory-based criterion for hydrometric network evaluation and design: Maximum information minimum redundancy. Water Resour Res 48(5). https://doi.org/10.1029/2011WR011251

Liu YB, De Smedt F (2004) WetSpa extension, a GIS-based hydrologic model for flood prediction and watershed management. Vrije Universiteit Brussel, Belgium 1:e108. https://www.vub.be/WetSpa/downloads/WetSpa_manual.pdf

Liu YB, De Smedt F (2005) Flood modeling for complex terrain using GIS and remote sensed information. Water Resour Manag 19(5):605–24. https://doi.org/10.1007/s11269-005-6808-x

Manandhar B, Balla MK, Awal R, Pradhan BM (2010) Floodplain analysis and risk assessment of lothar khola (stream). In Proceedings of the 11th ESRI India user conference, Noida, India, pp 21–22

Moghaddam DD, Rezaei M, Pourghasemi HR, Pourtaghie ZS, Pradhan B (2015) Groundwater spring potential mapping using bivariate statistical model and GIS in the Taleghan watershed, Iran. Arab J Geosci 8(2):913–29. https://doi.org/10.1007/s12517-013-11-561

Mouat DA, Mahin GG, Lancaster J (1993). Remote sensing techniques in the analysis of change detection. Geocarto Int 8(2):39–50. https://doi.org/10.1080/10106049309354407

Mukhopadhyay SC (2014) Aspects of hydro-geomorphology of north Bengal drainage, India and surroundings with emphasis on the Torsa basin. Indian J Landsc Syst Ecol Stud 37(2):163–176

Naghibi SA, Pourghasemi HR, Pourtaghi ZS, Rezaei A (2015) Groundwater qanat potential mapping using frequency ratio and Shannon's entropy models in the Moghan watershed, Iran. Earth Sci Inf 8(1):171–186. https://doi.org/10.1007/s12145-014-0145-7

Ozdemir A (2011). GIS-based groundwater spring potential mapping in the Sultan Mountains (Konya, Turkey) using frequency ratio, weights of evidence and logistic regression methods and their comparison. J Hydrol 411(3–4):290–308. https://doi.org/10.1016/j.jhydrol.2011.10.010

Ozdemir A, Altural T (2013) A comparative study of frequency ratio, weights of evidence and logistic regression methods for landslide susceptibility mapping: Sultan Mountains, SW Turkey. J As Earth Sci 64:180–97. https://doi.org/10.1016/j.jseaes.2012.12.014

Pourghasemi HR, Mohammady M, Pradhan B (2012) Landslide susceptibility mapping using index of entropy and conditional probability models in GIS: Safarood Basin, Iran. Catena 97:71–84. https://doi.org/10.1016/j.catena.2012.05.005

Pradhan B (2009) Groundwater potential zonation for basaltic watersheds using satellite remote sensing data and GIS techniques. Central Eur J Geosci 1(1):120–9. https://doi.org/10.2478/v10085-009-0008-5

Pradhan B, Lee S (2010) Landslide susceptibility assessment and factor effect analysis: backpropagation artificial neural networks and their comparison with frequency ratio and bivariate logistic regression modelling. Environ Modell Softw 25(6):747–59. https://doi.org/10.1016/j.envsoft.2009.10.016

Pradhan B, Shafiee M, Pirasteh S (2009) Maximum flood prone area mapping using RADARSAT images and GIS: Kelantan river basin. Int J Geoinf 5(2).

Rahmati O, Pourghasemi HR, Zeinivand H (2016) Flood susceptibility mapping using frequency ratio and weights-of-evidence models in the Golastan Province, Iran. Geocarto Int 31(1):42–70. https://doi.org/10.1080/10106049.2015.1041559

Rajsekhar D, Mishra AK, Singh VP (2013) Regionalization of drought characteristics using an entropy approach. J Hydrol Eng 18(7):870–87. https://doi.org/10.1061/(ASCE)HE.1943-5584.0000683

Regmi AD, Devkota KC, Yoshida K, Pradhan B, Pourghasemi HR, Kumamoto T, Akgun A (2014) Application of frequency ratio, statistical index, and weights-of-evidence models and their comparison in landslide susceptibility mapping in Central Nepal Himalaya. Arab J Geosci 7(2):725–742. https://doi.org/10.1007/s12517-012-0807-z

Sanyal J, Lu XX (2004) Application of remote sensing in flood management with special reference to monsoon Asia: a review. Nat Hazards 33(2):283–301. https://doi.org/10.1023/B:NHAZ.0000037035.65105.95

Shafapour Tehrany M, Kumar L, Neamah Jebur M, Shabani F (2019) Evaluating the application of the statistical index method in flood susceptibility mapping and its comparison with frequency ratio and logistic regression methods. Geomatics Nat Hazards Risk 10(1):79–101. https://doi.org/10.1080/19475705.2018.1506509

Skilodimou H, Livaditis G, Bathrellos G, Verikiou-Papaspiridakou E (2003) Investigating the flooding events of the urban regions of Glyfada and Voula, Attica, Greece: a contribution to Urban Geomorphology. Geografiska Annaler Ser A Phys Geogr 85(2):197–204. https://doi.org/10.1111/1468-0459.00198

Sujatha ER, Rajamanickam V, Kumaravel P, Saranathan E (2013) Landslide susceptibility analysis using probabilistic likelihood ratio model—a geospatial-based study. Arab J Geosci 6(2):429–40. https://doi.org/10.1007/s12517-011-0356-x

Swets JA (1988) Measuring the accuracy of diagnostic systems. Science 240(4857):1285–1293. https://doi.org/10.1126/science.3287615

Tehrany MS, Lee MJ, Pradhan B, Jebur MN, Lee S (2014) Flood susceptibility mapping using integrated bivariate and multivariate statistical models. Environ Earth Sci 72(10):4001–15. https://doi.org/10.1007/s12665-014-3289-3

Tehrany MS, Pradhan B, Jebur MN (2013) Remote sensing data reveals eco-environmental changes in urban areas of Klang Valley, Malaysia: contribution from object based analysis. J Indian Soc Remote Sens 41(4):981–91. https://doi.org/10.1007/s12524-013-0289-9

Tehrany MS, Pradhan B, Jebur MN (2015). Flood susceptibility analysis and its verification using a novel ensemble support vector machine and frequency ratio method. Stoch Environ Res Risk Assess 29(4):1149–65. https://doi.org/10.1007/s00477-015-1021-9

Tiwari MK, Chatterjee C (2010). Uncertainty assessment and ensemble flood forecasting using bootstrap based artificial neural networks (BANNs). J Hydrol 382(1–4):20–33. https://doi.org/10.1016/j.jhydrol.2009.12.013

Yilmaz I (2009) Landslide susceptibility mapping using frequency ratio, logistic regression, artificial neural networks and their comparison: a case study from Kat landslides (Tokat—Turkey). Comput Geosci 35(6):1125–38. https://doi.org/10.1016/j.cageo.2008.08.007

Yilmaz I (2010) Comparison of landslide susceptibility mapping methodologies for Koyulhisar, Turkey: conditional probability, logistic regression, artificial neural networks, and support vector machine. Environ Earth Sci 61(4):821–36. https://doi.org/10.1007/s12665-009-0394-9

Youssef S, Rosenberg E, Deschamps H, Oughanem R, Maire E, Mokso R (2014) Oil ganglia dynamics in natural porous media during surfactant flooding captured by ultra-fast x-ray microtomography. In Symposium of the society of core analysts. http://www.jgmaas.com/SCA/2014/SCA2014-023.pdf

Zare M, Pourghasemi HR, Vafakhah M, Pradhan B (2013) Landslide susceptibility mapping at Vaz Watershed (Iran) using an artificial neural network model: a comparison between multilayer perceptron (MLP) and radial basic function (RBF) algorithms. Arab J Geosci (8):2873–88. https://doi.org/10.1007/s12517-012-0610-x